A New Class of Heterobinuclear Complexes: Crystal Structure and Magnetism of Copper(II)-Nickel(II) Complexes Incorporating Two Different Macrocyclic Ligands

by **En-Qing Gao**[a]), **Jin-Kui Tang**[a]), **Dai-Zheng Liao***[a])[b]), **Zong-Hui Jiang**[a]), **Shi-Ping Yan**[a])[c]), and **Geng-Lin Wang**[a])

[a]) Department of Chemistry, Nankai University, Tianjin, 300071, P.R. China
[b]) State Key Laboratory of Structural Chemistry, Fujian Institute of Research on Structure of Matter, Chinese Academy of Sciences, Fuzhou, Fujian, 350002, P. R. China
[c]) State Key Laboratory of Chemistry and Application of Rare Earth Materials, Peking

Three novel oxamido-bridged heterobinuclear copper(II)-nickel(II) complexes incorporating two different tetraazamacrocyclic compounds were synthesized and characterized by IR, ESR, and electronic spectra. They are of the formulas $[(CuL^1)Ni(rac\text{-cth})](ClO)_{42}\cdot H_2O$ (**1**), $[Cu(L^2)Ni(rac\text{-cth})](ClO_4)_2\cdot 0.5$ EtOH (**2**), and $[(CuL^3)Ni(rac\text{-cth})](ClO_4)_2\cdot H_2O$ (**3**). L^1, L^2, and L^3 are the dianions of diethyl 5,6,7,8,16,17-hexahydro-6,7-dioxo-15*H*-dibenzo[*e*,*n*][1,4,8,12]tetraazacyclopentadecine-13,19-dicarboxylate, diethyl 5,6,7,8,15,16-hexahydro-6,7-dioxodibenzo[1,4,8,11]tetraazacyclotetracine-13,18-dicarboxylate, and diethyl 5,6,7,8,15,16-hexahydro-15-methyl-6,7-dioxodibenzo[1,4,8,11]tetraazacyclotetradecine-13,18-dicarboxylate, respectively, and *rac*-cth is *rac*-5,7,7,12,14,14-hexamethyl-1,4,8,11-tetraazacyclotetradecane. The crystal structures of **1** and **2** were determined by single-crystal X-ray analysis. The Ni^{II} ion is pseudooctahedrally coordinated. The coordination geometry around the Cu^{II} ion in **2** is slightly distorted square planar, while that in **1** shows significant distortion towards a tetrahedral structure. The temperature dependence of the magnetic susceptibility for **1** and **2** was analyzed by means of the Hamiltonian $\hat{\boldsymbol{H}} = -2J\hat{\boldsymbol{S}}_1\cdot\hat{\boldsymbol{S}}_2$, leading to $J = -63.9$ and $-67.4\ cm^{-1}$ for **1** and **2**, respectively.

Introduction. – The design and molecular magnetism of polynuclear complexes are of considerable interest for designing new magnetic materials and for investigating the structure and the role of the polymetallic active sites in biological systems [1–4]. One of the best strategies to design and synthesize polynuclear species is the 'complex as ligand' approach, *i.e.*, the use of mononuclear complexes that contain potential donor groups for another metal ion [1][5–10]. A good example of 'complex ligands' is represented by the mononuclear Cu^{II} complexes of *N*,*N*′-bis(coordinating-group)-substituted oxamides [6] such as [Cu(oxpn)] and $[Cu(obze)]^{2-}$ (*Fig. 1*). With these complexes as precursors, many oxamido-bridged polynuclear complexes have been prepared and studied magnetically in recent years [6–10]. The oxamido group has been noted as an efficient mediator of magnetic exchange between paramagnetic centers [1]. However, little work has been devoted to the design and magnetism of polynuclear species derived from macrocyclic oxamides, although metal complexes of macrocyclic ligands have been of great interest to coordination chemists for their special structures, properties, and/or functionalities [11][12]. Recently, we have reported several copper(II) complexes with $[15]N_4$ and $[14]N_4$ macrocyclic oxamides (*Fig. 1*, $[CuL^i]$, $i = 1-3$) [13][14]. Using these complexes as ligands, we have obtained a series of heterotetranuclear complexes of the type $[(CuL^i)_3M]$ (M = transition-metal

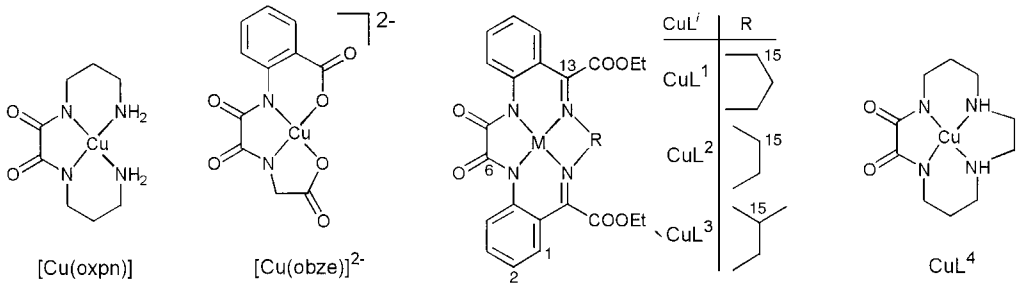

Fig. 1. *Some Cu^{II} complexes that have been used as ligands*

ions), some of which have been magnetically studied [13][15]. Very recently, *Robertson* and co-workers have reported the synthesis and magnetic properties of $[Cu^{II}_3]$ complexes derived from $[CuL^4]$ (*Fig. 1*) [16].

In continuation of our interest in polynuclear macrocyclic complexes, we present here a new class of heterobinuclear complexes that incorporate two different macrocyclic ligands. With the macrocyclic oxamidocopper(II) complexes $[CuL^i]$ ($i = 1-3$) as complex ligands and with another type of a tetraazamacrocyclic compound, *i.e.* *rac*-5,7,7,12,14,14-hexamethyl-1,4,8,11-tetraazacyclotetradecane (*rac*-cth), as the terminal ligand, the three $Cu^{II}Ni^{II}$ complexes $[(CuL^1)Ni(rac\text{-cth})](ClO_4)_2 \cdot H_2O$ (**1**), $[Cu(L^2)Ni(rac\text{-cth})](ClO_4)_2 \cdot 0.5$ EtOH (**2**), and $[(CuL^3)Ni(rac\text{-cth})](ClO_4)_2 \cdot H_2O$ (**3**) were prepared and characterized. The crystal structures and magnetic properties of **1** and **2** were investigated.

Results and Discussion. – *Description of the Structures. $[Cu(L^1)Ni($*rac*-cth$)](ClO_4)_2 \cdot H_2O$* (**1**). The structure of complex **1** consists of the heterobinuclear complex cations $[Cu(L^1)Ni(rac\text{-cth})]^{2+}$, H_2O molecules, and two sets of perchlorate ions. A perspective view of the binuclear cation with the weakly coordinated perchlorate ion is depicted in *Fig. 2*, and selected bond lengths and angles are listed in *Table 1*.

In the binuclear unit, the Cu- and Ni-atoms are bridged by an oxamido group. The Ni-atom assumes an asymmetrical distorted octahedral environment, with the two carbonyl O-atoms O(1) and O(2) of the macrocyclic oxamido ligand and the two N-atoms N(5) and N(7) of the macrocyclic tetraamine *rac*-cth in equatorial positions, and the other two N-atoms N(6) and N(8) of *rac*-cth in axial positions. The two axial Ni–N bonds are longer than the four equatorial bonds, as can be seen from *Table 1*. The rather small bite angle O(1)–Ni(1)–O(2) of 77.26° of the oxamido groups is the largest deviation from geometry of an octahedron. The Cu-atom resides in a highly distorted square-pyramidal surrounding with the two deprotonated oxamido N-atoms N(1) and N(3) (average Cu–N, 1.936 Å) and the two imino N-atoms N(2) and N(4) (average Cu–N, 1.957 Å) in basal positions. The apical position is occupied by a perchlorate O-atom (Cu(1)–O(7), 2.586 Å). The CuN_4 basal geometry is significantly distorted from square planar towards tetrahedral. The deviations of the four donor atoms from the their mean plane are 0.343 (N(1)), −0.320 (N(2)), −0.350 (N(3)), and 0.326 Å (N(4)), and the Cu-atom is 0.109 Å out of the plane. The tetrahedral distortion of the CuN_4 chromophore is even larger than that in the $[CuL^1]$ precursor [14]. The dihedral angle

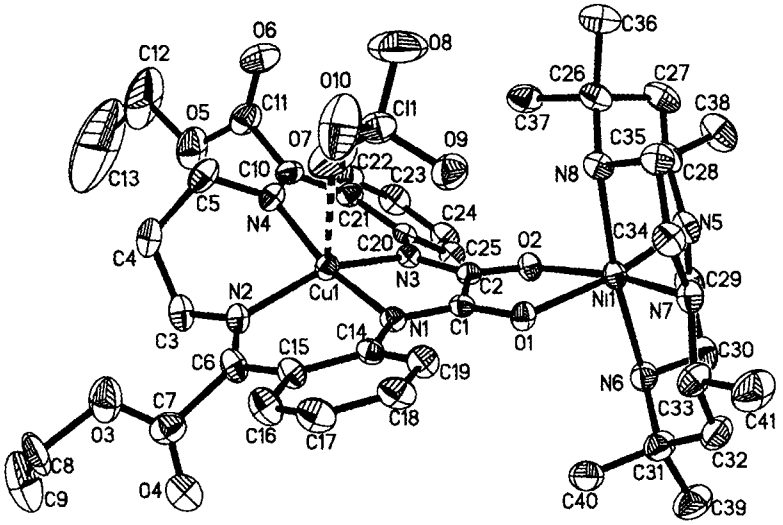

Fig. 2. *ORTEP View of the binuclear complex cation of* **1** *with the atom-numbering scheme*

Table 1. *Selected Bond Lengths* [Å] *and Angles* [°] *for* **1**

Cu(1)–N(3)	1.936(5)	Cu(1)–N(1)	1.937(5)
Cu(1)–N(4)	1.955(6)	Cu(1)–N(2)	1.958(5)
Ni(1)–O(2)	2.089(4)	Ni(1)–N(7)	2.098(5)
Ni(1)–O(1)	2.115(4)	Ni(1)–N(5)	2.122(6)
Ni(1)–N(6)	2.142(6)	Ni(1)–N(8)	2.149(5)
N(1)–C(1)	1.311(7)	N(3)–C(2)	1.318(8)
O(1)–C(1)	1.251(7)	O(2)–C(2)	1.243(7)
C(1)–C(2)	1.541(8)	Cu(1)–O(7)	2.586(6)
N(3)–Cu(1)–N(1)	86.2(2)	N(3)–Cu(1)–N(4)	93.1(2)
N(1)–Cu(1)–N(4)	166.1(2)	N(3)–Cu(1)–N(2)	153.6(2)
N(1)–Cu(1)–N(2)	95.0(2)	N(4)–Cu(1)–N(2)	91.9(2)
N(3)–Cu(1)–O(7)	106.7(2)	N(1)–Cu(1)–O(7)	84.3(2)
N(2)–Cu(1)–O(7)	99.7(3)	N(4)–Cu(1)–O(7)	82.6(2)
O(2)–Ni(1)–N(7)	166.96(19)	O(2)–Ni(1)–O(1)	77.26(16)
N(7)–Ni(1)–O(1)	89.76(19)	O(2)–Ni(1)–N(5)	91.7(2)
N(7)–Ni(1)–N(5)	101.3(2)	O(1)–Ni(1)–N(5)	168.5(2)
O(2)–Ni(1)–N(6)	89.2(2)	N(7)–Ni(1)–N(6)	91.3(2)
O(1)–Ni(1)–N(6)	97.5(2)	N(5)–Ni(1)–N(6)	85.8(2)
O(2)–Ni(1)–N(8)	95.74(19)	N(7)–Ni(1)–N(8)	84.8(2)
O(1)–Ni(1)–N(8)	87.77(19)	N(5)–Ni(1)–N(8)	89.9(2)
N(6)–Ni(1)–N(8)	173.5(2)		

between the Ni equatorial plane and the Cu basal plane is 29.1°. The Cu- and Ni-atoms are separated by 5.29 Å and displaced towards the same side of the $C_2O_2N_2$ bridge plane by 0.346 and 0.342 Å, respectively. The average C–O and C–N bond lengths in the oxamido group of **1** are 1.247 and 1.314 Å, respectively, while the corresponding distances for the mononuclear [CuL^1] precursor are 1.211 and 1.355 Å, respectively [14]. The increase in the C–O and the decrease in the C–N distances in the binuclear

complex reflect the delocalization of the electron density from the N-atoms towards the O-atoms upon the coordination of the O-atoms to Ni^{II}.

*[Cu(L²)Ni(*rac*-cth)](ClO₄)₂·0.5 EtOH* (**2**). The structure of complex **2** consists of the heterobinuclear complex cations $[Cu(L^2)Ni(\textit{rac}\text{-cth})]^{2+}$, uncoordinated perchlorate ions, and disordered EtOH molecules. A perspective view of the binuclear unit is depicted in *Fig. 3*, and selected bond lengths and angles are listed in *Table 2*.

The coordination environment of the Ni-atom in **2** is similar to that in **1**. The bite angle O(1)–Ni(1)–O(2) of the oxamido group is 77.70°. However, as can be seen from *Tables 1* and *2*, the chelating mode of the oxamido group in **2** is more unsymmetric, with the Ni(1)–O(1) distance (2.130(2) Å) being significantly longer than Ni(1)–O(2) (2.075(3) Å). The Cu-atom resides in the coordination cavity formed by the four N-donors of the $[14]N_4$ macrocyclic oxamide, with a slightly distorted square-planar geometry. The deviations of donor atoms from the N_4 mean plane are ±0.082 Å for N(1) and N(2) and ±0.083 Å for N(3) and N(4), and the Cu-atom is 0.052 Å out of the plane. These values are very close to those for the $[CuL^2]$ precursor [14] and much smaller than those in **1** and $[CuL^1]$. The dihedral angle between the equatorial NiN_2O_2 and the CuN_4 mean planes is 43.6°. The Cu- and Ni-atoms are displaced towards the same side of the bridge plane by 0.575 and 0.464 Å. These distances are larger than those in **1**. The Cu···Ni separation is 5.177 Å. As has been observed for **1** and $[CuL^1]$, on going from $[CuL^2]$ to **2**, the C–O (oxamido) and C–N (oxamido) distances increase (from 1.213 to 1.248 Å) and decrease (from 2.356 to 2.329 Å), respectively.

IR and Electronic Spectra. The IR spectra of the three complexes are very similar. The very sharp medium-intensity band at 3225–3250 cm^{-1} and the broad strong band at

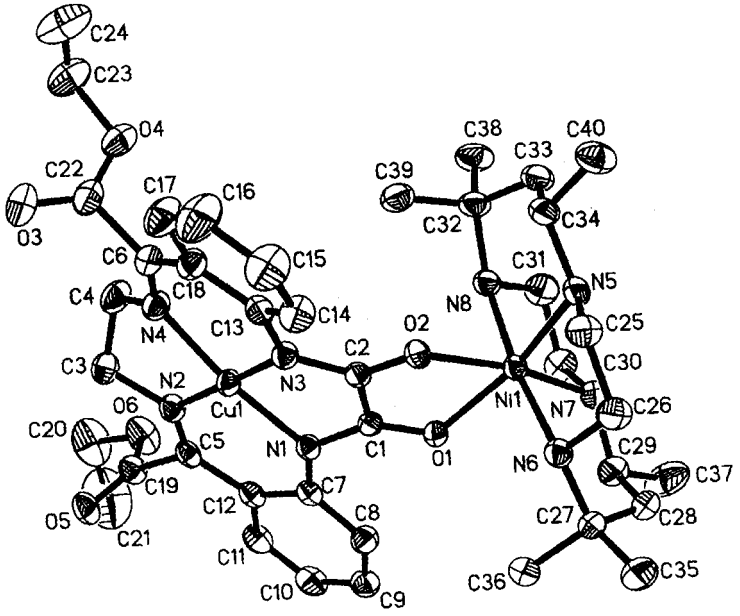

Fig. 3. *ORTEP View of the binuclear complex cation of* **2** *with the atom-numbering scheme*

Table 2. *Selected Bond Lengths* [Å] *and Angles* [°] *for* **2**

Ni(1)–O(2)	2.075(3)	Ni(1)–O(1)	2.130(2)
Ni(1)–N(7)	2.088(3)	Ni(1)–N(5)	2.107(3)
Ni(1)–N(8)	2.153(4)	Ni(1)–N(6)	2.159(4)
Cu(1)–N(1)	1.935(3)	Cu(1)–N(3)	1.923(3)
Cu(1)–N(2)	1.939(3)	Cu(1)–N(4)	1.945(3)
O(1)–C(1)	1.246(4)	O(2)–C(2)	1.251(4)
N(1)–C(1)	1.331(5)	N(3)–C(2)	1.327(5)
N(2)–C(5)	1.278(5)	N(4)–C(6)	1.278(6)
C(1)–C(2)	1.536(5)		
O(2)–Ni(1)–O(1)	77.70(9)	N(7)–Ni(1)–N(5)	103.12(15)
N(5)–Ni(1)–O(1)	166.89(13)	N(7)–Ni(1)–O(1)	89.94(12)
O(2)–Ni(1)–N(7)	167.63(12)	O(2)–Ni(1)–N(5)	89.24(12)
O(1)–Ni(1)–N(6)	96.72(12)	O(1)–Ni(1)–N(8)	88.60(13)
O(2)–Ni(1)–N(8)	94.98(13)	N(7)–Ni(1)–N(8)	84.84(14)
N(5)–Ni(1)–N(8)	91.33(14)	O(2)–Ni(1)–N(6)	89.56(14)
N(7)–Ni(1)–N(6)	91.71(15)	N(5)–Ni(1)–N(6)	84.13(13)
N(8)–Ni(1)–N(6)	173.54(15)		
N(3)–Cu(1)–N(1)	86.79(13)	N(3)–Cu(1)–N(2)	177.52(14)
N(1)–Cu(1)–N(2)	95.00(14)	N(3)–Cu(1)–N(4)	92.38(14)
N(1)–Cu(1)–N(4)	172.01(14)	N(2)–Cu(1)–N(4)	86.09(15)

ca. 1080 cm^{-1} are characteristic of the NH group in *rac*-cth [17] and the perchlorate ion [18], respectively. The bands at *ca.* 1730 and 1630 cm^{-1}, which show no significant shift relative to the corresponding bands of the mononuclear [CuL^i] complexes ($i = 1-3$), are attributed to $\tilde{\nu}$(C=O) (ester) and $\tilde{\nu}$(C=N), respectively [13]. The strong $\tilde{\nu}$(C=O) (oxamido) band at *ca.* 1650 cm^{-1} in the spectra of the mononuclear precursors [13] is replaced by a strong band at *ca.* 1575 cm^{-1} in the spectra of the binuclear complexes. The significant bathochromic shift is consistent with the decrease in the C=O bond lengths on coordination, as confirmed by the X-ray crystallographic studies.

The electronic-absorption spectra of the three binuclear complexes in MeCN below 500 nm are dominated by intense bands due to intraligand and charge-transfer transitions in the Cu^{II} chromophore [14]. In the 500–1000 nm region, they exhibit two broad bands: *i*) the weak near-IR absorption ($\varepsilon = 37-50$ M^{-1} cm^{-1}) centered at 935, 940, and 935 nm for **1**, **2**, and **3**, respectively, are assignable to the $^3A_{2g}(Ni) \rightarrow {}^3T_{2g}(Ni)$ transitions, assuming an O_h site symmetry for Ni^{II} [9]; *ii*) a relatively stronger band centered at 630 nm ($\varepsilon = 245$ M^{-1} cm^{-1}) was observed for **1**, and can be attributed to the envelope of the *d-d* transitions of Cu^{II} in an environment that is nearly square planar. The corresponding *d-d* bands for **2** and **3** appear at 560 and 540 nm (ε *ca.* 300 M^{-1} cm^{-1}), respectively, as shoulders of the charge-transfer bands. The significant red shift in the maximum of the *d-d* (Cu) band for **1** relative to those for **2** and **3** is in agreement with the significant tetrahedral distortion of the CuN_4 chromophore in **1** [14][19]. The other two spin-allowed transitions for the pseudo-octahedral Ni^{II} chromophore are obscured by the *d-d* and charge-transfer bands due to the Cu^{II} chromophore.

ESR Spectra. The polycrystalline X-band ESR spectra were measured at room temperature (*Fig. 4*). The *g* parameters are listed in *Table 3*. The three complexes present very similar behaviors, exhibiting a broad intense band centered at $g \approx 2.17$ and a broad signal with the maximum at $g = 5.02-5.50$. The antiferromagnetic interaction

in $Cu^{II}Ni^{II}$ pairs gives rise to an $S=1/2$ ground state and $S=3/2$ excited state. The allowed $|1/2, -1/2\langle \rightarrow |1/2, 1/2\langle$ transition in the doublet state will exhibit a resonance at a field corresponding approximately to $g=2$. On the other hand, the zero-field splitting of the quartet state gives rise to two *Kramer*'s doublets $|3/2, \pm 1/2\langle$ and $|3/2, \pm 3/2\langle$. Assuming that the zero-field splitting is axial, the allowed transition within the $|3/2, \pm 1/2\langle$ doublet will produce two resonant signals: one near $g=2$ and the other at approximately half-field with $g>4$ [9]. According to magnetic studies (*vide infra*), the doublet-quartet gap $|3J|$ (*ca.* 200 cm^{-1}) is comparable to the kT value at room temperature (*ca.* 205 cm^{-1}), suggesting that the excited state is significantly populated. The signals of the quartet state are superimposed on that of the doublet state to produce the observed spectra.

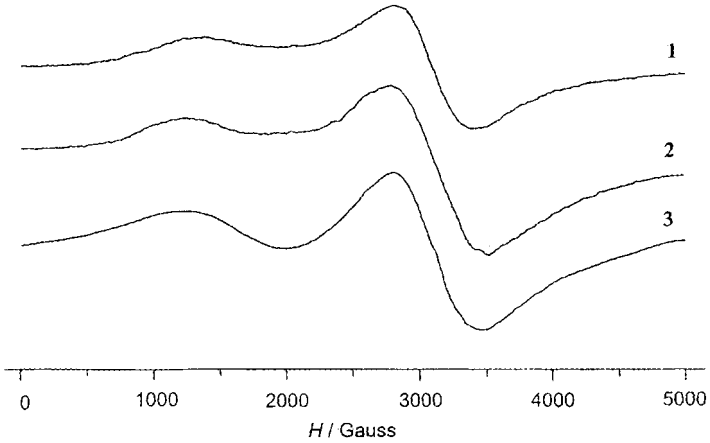

Fig. 4. *Polycrystalline X-band ESR spectra of complexes* **1**–**3** *at room temperature*

Table 3. *Parameters Obtained from ESR and Magnetic Analyses*

	ESR		Magnetic analyses			
	g_1	g_2	J/cm^{-1}	g_{Cu}	g_{Ni}	$R^a)$
1	2.17	5.02	– 63.9	2.11	2.23	2.72×10^{-4}
2	2.15	5.40	– 67.4	2.10	2.19	2.60×10^{-4}
3	2.17	5.50	–	–	–	–

[a]) $R=\Sigma\,(\chi_{obs.}-\chi_{calc.})^2/\Sigma\,\chi^2_{obs.}$.

Magnetic Properties. The temperature dependence of the molar magnetic susceptibility (χ_M) and its product with temperature ($\chi_M T$) for **1** and **2** are shown in *Fig. 5*. The $\chi_M T$ products at room temperature are 1.25 and 1.20 $cm^3\ mol^{-1}$ K for **1** and **2**, respectively, below the spin-only value (1.38 $cm^3\ mol^{-1}$ K) expected for an uncoupled $Cu^{II}Ni^{II}$ system. The product for each compound decreases as the temperature is lowered, and finally reaches a plateau below *ca.* 40 K, with $\chi_M T \approx 0.47-0.49$ $cm^3\ mol^{-1}$ K, respectively. These features are quite typical of isolated $Cu^{II}Ni^{II}$ pairs with antiferromagnetic intramolecular interaction. The plateaus indicate that only the doublet ground state is thermally populated at low temperature.

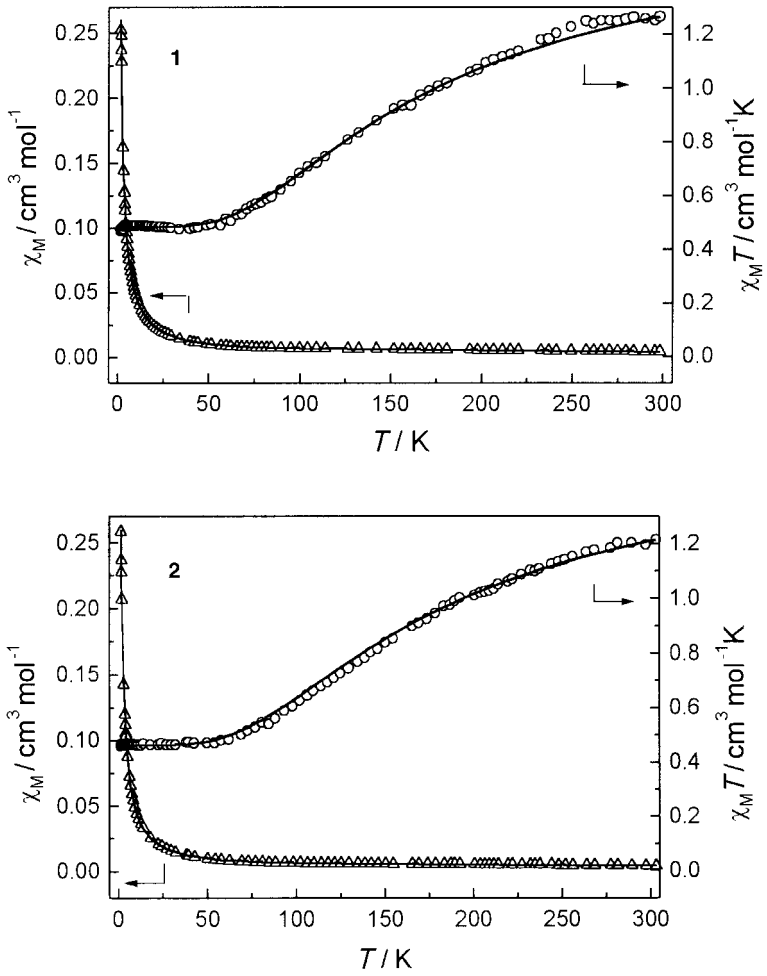

Fig. 5. χ_M vs. T (△) *and* χ_MT vs. T (○) *plots for complexes* **1** *and* **2**

The magnetic data were fitted on the basis of the isotropic *Heisenberg* model $\hat{\boldsymbol{H}} = -2J\hat{\boldsymbol{S}}_1 \cdot \hat{\boldsymbol{S}}_2$, where $\boldsymbol{J}$ is the interaction parameter between two paramagnetic centers. For $Cu^{II}Ni^{II}$ complexes, the theoretical expression of the magnetic susceptibility is given by *Eqn. 1*, where the g_s ($S = 1/2$, 3/2) factors are related to local g factors by $g_{1/2} = (4g_{Ni} - g_{Cu})/3$ and $g_{3/2} = (2g_{Ni} + g_{Cu})/3$. The simulations of the experimental complexes based on the above expression are quite satisfactory, as shown in *Fig. 5*. The parameters obtained are listed in *Table 3*.

$$\chi_M = \frac{N\beta^2}{4kT} \left[\frac{g_{1/2}^2 + 10g_{3/2}^2 \exp(3J/kT)}{1 + 2\exp(3J/kT)}\right] \quad (1)$$

According to *Kahn* [1], the antiferromagnetic interaction between Cu^{II} and Ni^{II} arises from the non-zero overlap between the $d_{x^2-y^2}$ magnetic orbitals centered on the two metal ions and delocalized towards ligands. The larger the overlap, the stronger the

interaction. From X-ray crystallographic studies, the structures of the two binuclear complexes differ mainly in two aspects: *i*) the CuN_4 moiety in **1** exhibits much more significant distortion towards tetrahedral than that in **2**. *ii*) The distances from metal ions to the oxamido bridge plane in **1** are significantly shorter than those in **2**. The significant distortion of the CuN_4 moiety in **1** disfavors the delocalization of the Cu^{II} magnetic orbital and is expected to result in a weaker antiferromagnetic interaction than that in **2**. However, the shorter distances from the metal ions to the bridge plane in **1** have opposite effects. The compromise between the two conflicting factors results in comparable J values for the two complexes. The slightly smaller $|J|$ value for **1** may suggest that the former factor dominates the latter.

Conclusion. – Three novel oxamido-bridged heterobinuclear $Cu^{II}Ni^{II}$ complexes incorporating two different tetraazamacrocyclic compounds were synthesized and characterized by IR, ESR, and electronic spectra. The crystal structures of **1** and **2** were determined by single-crystal X-ray analysis. The Ni^{II} ion is pseudooctahedrally coordinated. The coordination geometry around the Cu^{II} ion in **2** is slightly distorted square planar, while that in **1** shows significant distortion towards tetrahedral. The temperature dependence of the magnetic susceptibility for **1** and **2** was analyzed by the Hamiltonian $\hat{\boldsymbol{H}} = -2J\hat{\boldsymbol{S}}_1 \cdot \boldsymbol{S}_2$, leading to $J = -63.9$ and -67.4 cm^{-1} for **1** and **2**, respectively.

Experimental Part

General. All chemicals were of A. R. grade and used as received. The mononuclear precursors, [CuL^1], [CuL^2], [CuL^3] [13], and [Ni(*rac*-cth)]$(ClO_4)_2$ [20] were prepared as described elsewhere. Electronic spectra: *Shimadzu-UV-365* UV-VIS-NR spectrophotometer; in MeCN. X-Band ESR spectra: *Bruker ER-200-D-SRC* ESR spectrometer. IR Spectra: *Shimadzu IR-408* spectrometer; KBr pellets; only main bands are given; in cm^{-1}. Variable-temperature magnetic susceptibilities: *Maglab-2000* vibrating sample magnetometer; diamagnetic corrections were made with *Pascal*'s constants for all the constituent atoms [21]. Elemental analyses (C, H, N): *Perkin-Elmer 240* analyzer.

*Copper{μ-{diethyl 5,6,7,8,16,17-Hexahydro-6,7-di(oxo-κO)-15*H*-dibenzo[*e,n*][1,4,8,12]tetraazacyclopentadecine-13,19-dicarboxylato(2−)-κ*N^6,κN^8,κN^{14},κN^{18}*}}(5,7,7,12,14,14-hexamethyl-1,4,8,11-tetraazacyclotetradecane-κ*N^1,κN^4,κN^8,κN^{11}*)nickel(2+) Diperchlorate Hydrate* ([(CuL^1)Ni(*rac*-cth)]$(ClO_4)_2 \cdot H_2O$; **1**). To a suspension of [CuL^1] (0.162 g, 0.3 mmol) in 95% EtOH/H_2O (20 ml) was added a solid sample of [Ni(*rac*-cth)]$(ClO_4)_2$ (0.163 g, 0.3 mmol). The mixture was stirred under reflux for 3 h and then left to cool. The resulting precipitate was filtered off and dissolved in MeCN/EtOH/BuOH 2:1:1. Slow evaporation of the soln. afforded red crystals. IR (KBr): 3400*w* (br.), 3250*m*, 2960*m*, 1735*s*, 1630 (sh), 1605*s*, 1576*s*, 1560*m*, 1482*m*, 1440*m*, 1348*s*, 1192*m*, 1168*m*, 1085v*s*, 853*w*, 815*w*, 770*w*, 750*s*. Anal. calc. for $C_{41}H_{62}Cl_2CuN_8NiO_{15}$: C 44.76, H 5.68, N 10.18; found: C 44.30, H 5.84, N 10.18.

*Copper{*μ*-{diethyl 5,6,7,8,15,16-Hexahydro-6,7-di(oxo-*κO*)dibenzo[*f,l*][1,4,8,11]tetraazacyclotetradecine-13,18-dicarboxylato(2−)-*κN^5,κN^8,κN^{14},κN^{17}*}}(5,7,7,12,14,14-hexamethyl-1,4,8,11-tetraazacyclotetradecane-*κN^1,κN^4,κN^8,κN^{11}*)nickel(2+) Diperchlorate Compound with Ethanol* ([($Cu(L^2)$Ni(*rac*-cth)]$(ClO_4)_2 \cdot 0.5$ EtOH; **2**). As described for **1**, with [CuL^2] instead of [CuL^1]. IR (KBr): 3400*w* (br.), 3225*m*, 2940*m*, 1730*s*, 1622*s*, 1598*s*, 1575*s*, 1552*m*, 1465*m*, 1440*m*, 1342*s*, 1200*s*, 1165*m*, 1075v*s* (br.), 854*w*, 815*w*, 765*w*, 745*m*. Anal. calc. for $C_{41}H_6Cl_2CuN_8NiO_{14.5}$: C 45.13, H 5.63, N 10.27; found: C 44.74, H 5.91, N 10.02.

*Copper{*μ*-{diethyl 5,6,7,8,15,16-Hexahydro-15-methyl-6,7-di(oxo-*κO*)dibenzo[*f,l*][1,4,8,11]tetraazacyclotetradecine-13,18-dicarboxylato(2−)-*κN^5,κN^8,κN^{14},κN^{17}*}}(5,7,7,12,14,14-hexamethyl-1,4,8,11-tetraazacyclotetradecane-*κN^1,κN^4,κN^8,κN^{11}*)nickel(2+) Diperchlorate Hydrate* ([(CuL^3)Ni(*rac*-cth)]$(ClO_4)_2 \cdot H_2O$; **3**). As described for **1**, with [CuL^3] instead of [CuL^1], but all efforts to grow single crystals failed. IR (KBr): 3400*w* (br.), 3225*m*, 2940*m*, 1740*s*, 1620 (sh), 1600*s*, 1575*s*, 1550*m*, 1475*m*, 1440*m*, 1340*s*, 1195*s*, 1165*m*, 1080v*s* (br.), 850*w*, 815*w*, 768*w*, 750*s*. Anal. calc. for $C_{41}H_{62}Cl_2CuN_8NiO_{15}$: C 44.76, H 5.68, N 10.18; found: C 45.01, H 5.64, N 10.29.

Crystallography. Intensity data for single crystals of complex **1** and **2** were collected on a *Bruker Smart-1000-CCD* area detector. The structures were solved by direct methods and subsequent *Fourier* difference

techniques, and refined anisotropically by full-matrix least squares on F^2 [22]. Crystal data and structure refinements are summarized in *Table 4*. Crystallographic data (excluding structure factors) for the structures reported in this paper have been deposited with the *Cambridge Crystallographic Data Centre* as supplementary publication No. CCDC-150001 (**1**) and -150002 (**2**). Copies of the data can be obtained free of charge on application to CCDC, 12 Union Road, Cambridge CB2 1EZ, UK (fax: +44-1223/336-033; e-mail: deposit@ccdc.cam.ac.uk).

Table 4. *Crystal Data for [Ni(CuL^1)] Complex* **1** *and [Ni(CuL^2)] Complex* **2**

	1	**2**
Formula	$C_{41}H_{62}Cl_2CuN_8NiO_{15}$	$C_{41}H_{61}Cl_2CuN_8NiO_{14.50}$
Formula weight	1100.14	1091.13
Crystal system	Monoclinic	Triclinic
Space group	$P2_1/n$	$P\bar{1}$
a [Å]	15.2129(15)	12.4504(8)
b [Å]	16.0215(15)	13.8719(8)
c [Å]	21.820(2)	15.8657(9)
α [°]	90	90.2520(10)
β [°]	103.081(2)	111.9910(10)
γ [°]	90	102.2900(10)
V [Å^3]	5180.2(8)	2471.9(3)
Z	4	2
μ(MoK_α)/cm^{-1}	14.11	9.91
T/K	298(2)	293(2)
Reflections measured	18149	10334
Unique reflections	9026	8652
R(int)	0.0687	0.0298
R_1, wR_2 ($I > 2\sigma(I)$)	0.0661, 0.1570	0.0542, 0.1528
R_1, wR_2 (all data)	0.1532, 0.2069	0.0689, 0.1682

This work was supported by the *Natural Science Foundation of China* (No. 20071019).

REFERENCES

[1] O. Kahn, 'Molecular Magnetism', New York, VCH Publishers, 1993; O. Kahn, *Struct. Bonding* **1987**, *68*, 89; O. Kahn, *Adv. Inorg. Chem.* **1996**, *4*, 179.
[2] S. Miller, A. J. Epstein, *Chem. Eng. News* **1995**, Oct. 2, 30.
[3] 'Molecular Magnetic Materials, Eds. D. Gatteschi, O. Kahn, J. S. Miller, F. Palacio, NATO ASI Series, Kluwer, Dordrecht, The Netherlands, 1991.
[4] B. J. Wallar, J. D. Lipscomb, *Chem. Rev.* **1996**, *96*, 2625; E. I. Solomon, T. C. Brunold, M. Z. Davis, J. N. Kemsley, S.-K. Lee, N. Lehnert, A. J. Skulan, Y. S. Yang, J. Zhou, *Chem. Rev.* **2000**, *100*, 235.
[5] See, *e.g.*, S. J. Gruber, C. M. Harris, E. Sinn, *J. Inorg. Nucl. Chem.* **1968**, *30*, 1805; N. B. O'Brien, T. O. Maier, I. C. Paul, R. S. Drago, *J. Am. Chem. Soc.* **1973**, *95*, 6640.
[6] H. Ojima, K. Nonoyama, *Coord. Chem. Rev.* **1988**, *92*, 85; R. Ruiz, J. Faus, F. Lloret, M. Julve, Y. Journaux, *Coord. Chem. Rev.* **1999**, *193–195*, 1069.
[7] J. L. Sanz, R. Ruiz, A. Gleizes, F. Lloret, J. Faus, M. Julve, J. J. Borrás-Almenar, Y. Journaux, *Inorg. Chem.* **1996**, *35*, 7384; Z.-Y. Zhang, D.-Z. Liao, Z.-H. Jiang, S.-Q. Hao, X.-K. Yao, H.-G. Wang, G.-L. Wang, *Inorg. Chim. Acta* **1990**, *173*, 201; J. Larionova, S. A. Chavan, J. V. Yakhmi, A. G. Frøystein, J. Sletten, C. Sourisseau, O. Kahn, *Inorg. Chem.* **1997**, *36*, 6374.
[8] F. Lloret, Y. Journaux, M. Julve, *Inorg. Chem.* **1990**, *29*, 3967; C. Mathoniére, O. Kahn, J. C. Daran, H. Hilbig, F. H. Köhler, *Inorg. Chem.* **1993**, *32*, 4057; K. Nakatani, J. Y. Carriat, Y. Journaux, O. Kahn, F. Lloret, J. P. Renard, Y. Pei, J. Sletten, M. Verdaguer, *J. Am. Chem. Soc.* **1989**, *111*, 5739; F. Lloret, M. Julve, R. Ruiz, Y. Journaux, K. Nakatani, O. Kahn, J. Sletten, *Inorg. Chem.* **1993**, *32*, 27.

[9] A. Escuer, R. Vicente, J. Ribas, R. Costa, X. Solans, *Inorg. Chem*. **1992**, *31*, 2627; L. Banci, A. Bencini, C. Benelli, D. Getteschi, *Inorg. Chem*. **1981**, *20*, 1399.
[10] D. Christodoulou, M. G. Kanatzidis, D. Coucouvanis, *Inorg. Chem.* **1990**, *29*, 191.
[11] 'Coordination Chemistry of Macrocyclic Compounds', Ed. G. A. Melson, Plenum, New York, 1979.
[12] C. T. Chen, K. S. Suslick, *Coord. Chem. Rev.* **1993**, *128*, 293; P. A. Vigato, S. Tamburini, D. E. Fenton, *Coord. Chem. Rev.* **1990**, *106*, 25.
[13] E.-Q. Gao, G.-M. Yang, D.-Z. Liao, Z.-H. Jiang, S.-P. Yan, G.-L. Wang, H.-Z. Kou, *Trans. Met. Chem*. **1999**, *24*, 244.
[14] E.-Q. Gao, W.-M. Bu, G.-M. Yang, D.-Z. Liao, Z.-H. Jiang, S.-P. Yan, G.-L. Wang, *J. Chem. Soc., Dalton Trans.* **2000**, 1431.
[15] E.-Q. Gao, G.-M. Yang, D.-Z. Liao, Z.-H. Jiang, S.-P. Yan, G.-L. Wang, *J. Chem. Res. (S)* **1999**, 278; E.-Q. Gao, G.-M. Yang, J.-K. Tang, D.-Z. Liao, Z.-H. Jiang, S.-P. Yan, *Polyhedron* **1999**, *18*, 3643.
[16] L. Cronin, A. R. Mount, S. Parsons, N. Robertson, *J. Chem. Soc., Dalton Trans.* **1999**, 1925.
[17] N. F. Curtis, *J. Chem. Soc., Dalton Trans.* **1964**, 2644.
[18] K. Nakamoto, 'Infrared and Raman Spectra of Inorganic and Coordination Compounds', John Wiley, New York, 5th edn., 1997, Part B, p. 83.
[19] H. Yokoi, *Bull. Chem. Soc. Jpn*. **1974**, *47*, 3037.
[20] A. M. Tait, D. H. Bush, *Inorg. Synth.* **1978**, *18*, 10.
[21] P. W. Selwood, 'Magnetochemistry', Interscience, New York, 1956, p. 78.
[22] G. M. Sheldrick, 'SHELXS-97 and SHELXL-97, Software for Crystal Structure Analysis', Siemens Analytical X-Ray Instruments Inc., Wisconsin, Madison, USA, 1997.

Received December 27, 2000